AIP | Review of Scientific Instruments

Raman calibration of the LHD YAG Thomson scattering for electron-density measurements

I. Yamada, K. Narihara, and H. Hayashi

Citation: Rev. Sci. Instrum. **74**, 1675 (2003); doi: 10.1063/1.1538362

View online: http://dx.doi.org/10.1063/1.1538362

View Table of Contents: http://rsi.aip.org/resource/1/RSINAK/v74/i3

Published by the American Institute of Physics.

Related Articles

Single exposure three-dimensional imaging of dusty plasma clusters
Rev. Sci. Instrum. 84, 023501 (2013)

Hydrogen transport diagnostics by atomic and molecular emission line profiles simultaneously measured for large helical device
Phys. Plasmas 20, 012514 (2013)

Time-and-space resolved comparison of plasma expansion velocities in high-power diodes with velvet cathodes
J. Appl. Phys. 113, 043307 (2013)

Development of a diffuse air-argon plasma source using a dielectric-barrier discharge at atmospheric pressure
Appl. Phys. Lett. 102, 033503 (2013)

Nonmonotonic radial distribution of excited atoms in a positive column of pulsed direct currect discharges in helium
Appl. Phys. Lett. 102, 034104 (2013)

Additional information on Rev. Sci. Instrum.

Journal Homepage: http://rsi.aip.org

Journal Information: http://rsi.aip.org/about/about_the_journal

Top downloads: http://rsi.aip.org/features/most_downloaded

Information for Authors: http://rsi.aip.org/authors

ADVERTISEMENT

Raman calibration of the LHD YAG Thomson scattering for electron-density measurements

I. Yamada,[a] K. Narihara, H. Hayashi, and LHD Experimental Group
National Institute for Fusion Science, 322-6 Oroshi-Cho, Toki-City Gifu-Ken 509-5292, Japan

(Presented on 8 July 2002)

We have calibrated the LHD yttrium aluminum garnet (YAG) Thomson scattering system by using anti-Stokes rotational Raman scattering from air for the measurements of absolute electron-density profiles of LHD plasmas. The air Raman calibration was carried out at near atmospheric pressure and room temperature. Total uncertainty in measured electron densities is estimated to be ±15% or less. Electron densities obtained with the calibrated YAG Thomson scattering show good agreements with those measured by the LHD millimeter-wave interferometer. © *2003 American Institute of Physics.* [DOI: 10.1063/1.1538362]

I. INTRODUCTION

The Thomson scattering system is one of the most reliable diagnostics for the measurements of electron temperature and density profiles of fusion plasmas. For electron-density measurements, the Thomson scattering system should be absolutely calibrated. The absolute calibrations using rotational Raman scatterings from gaseous hydrogen and nitrogen have been proposed and applied.[1,2] The hydrogen Raman calibration may be more convenient because the wavelength shifts are larger and the scattering characteristics have been well established. However, filling huge fusion devices like LHD with a large amount of gaseous hydrogen is very dangerous and not recommended from a safety point of view. Accurate data on the Raman cross section and wavelength shift for molecular nitrogen and oxygen have been also reported as well as gaseous hydrogen. Therefore, we have calibrated the LHD yttrium aluminum garnet (YAG) Thomson scattering system by using the rotational Raman scatterings from air ($N_2:O_2=78\%:21\%$). In this article, we describe the calibration procedure and error estimation, and show some examples of electron temperature and density profiles measured by the calibrated LHD Thomson scattering.

II. RAMAN CALIBRATION

The experimental setup is identical in both the Thomson and Raman scattering measurements, except that the LHD vacuum vessel is filled with air in the Raman calibration. A detailed description of the LHD YAG Thomson scattering system is given in previous papers.[3,4] The Thomson scattering uses several YAG lasers and Thomson scattered light is analyzed with polychromators that have five wavelength channels. Figures 1 and 2 show the spectral responsibilities of a polychromator together with the Thomson spectrum and effective cross-section distributions of the rotational Raman lines for molecular nitrogen and oxygen, respectively. Since the effective cross section of Raman scattering falls exponentially as the wavelength shift increases, the Raman signals can be detected by only channel 1 in the polychromators. Signal intensity of Thomson scattering detected by channel 1, S^T, is written as

$$S^T = AL n_e \int \sigma^T(T_e,\lambda) f_1(\lambda) d\lambda \frac{dI^T}{d\Omega}, \tag{1}$$

where A is the whole instrumental coefficient that is identical in both Thomson and Raman measurements, L is the pulse energy of incident laser, n_e is the electron density, σ^T is the cross section of Thomson scattering, f_1 is the spectral responsibility of the channel 1, and $dI^T/d\Omega$ is the angular distribution of Thomson light

$$\frac{dI^T}{d\Omega} = \frac{3}{8\pi}\sin^2\beta, \tag{2}$$

where β is the angle between the polarization of incident laser and observation direction. The coefficient A includes the solid angle, scattering length, and other optical efficiencies of optics used such as the transmissivity of the view window. We use the Thomson spectrum that includes the second-order relativistic effect to evaluate $\int \sigma^T(T_e,\lambda) f_1(\lambda) d\lambda$.[5] A similar equation is given for Raman signal S^R:

$$S^R = AL\left[n^N \sum_J w_J^N \sigma_J^N(\lambda_J^N) f_1(\lambda_J^N) + n^O \sum_J w_J^O \sigma_J^O(\lambda_J^O) f_1(\lambda_J^O)\right]\frac{dI^R}{d\Omega}, \tag{3}$$

where J is the initial rotational-angular-momentum quantum number, $w_J^{N,O}$ is the population of the initial rotational state, $\sigma_J^{N,O}$ is the cross section of the anti-Stokes rotational $J'=J-2$ Raman transition, and "N" and "O" stand for nitrogen and oxygen, respectively. The values of $w_J^{N,O}$, $\sigma_J^{N,O}$, and $\lambda_J^{N,O}$ are evaluated as follows.[6–8] Necessary molecular constants are listed for molecular nitrogen and oxygen in Table I. The Raman shifted wavelength, $\lambda_J^{N,O}$ can be calculated from the wave-number shift, $\delta\nu=(4B_0-6D_0)(J-1/2)-8D_0(J$

[a]Electronic mail: yamadai@nifs.ac.jp

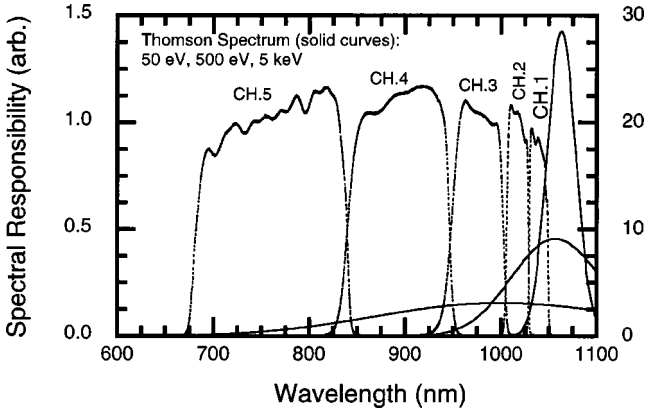

FIG. 1. Spectral responsibility of a five channel polychromator (dashed curves) and Thomson spectrum (solid curves).

$-1/2)$.[3] The population of the initial rotational state J in thermal equilibrium at a temperature T is given by[6,7]

$$w_J^{N,O} = W^{-1} g_J (2J+1) \exp[-J(J+1) hcB_0/kT], \tag{4}$$

where g_J is the statistical weight factor depending on the nuclear spin. Normalization factor W is determined from

$$\sum_{J=0}^{\infty} w_J = 1. \tag{5}$$

The differential cross section of rotational Raman scatterings is written as

$$\sigma_J^R = \sigma_{zz}[(1-\rho)\cos^2\psi + \rho], \tag{6}$$

$$\sigma_{zz} = \frac{64\pi^4}{45} \frac{3J(J+1)}{2(2J+1)(2J-1)} \frac{\gamma^2}{\lambda_J^4}, \tag{7}$$

where ρ is the depolarization factor, ψ is the angle between the polarizations of incident and scattered lights, and γ is the polarizability anisotropy.[6] The Raman-scattered light is largely unpolarized and the theoretical value of the depolarization ρ is 3/4. The values of polarizability anisotropy are estimated at the incident wavelength of 1064 nm by linear extrapolation from experimental data.[6,9,10] and listed in Table I. The angular dependence of the differential cross section for the quadrupole Raman transition differs from that of dipole Thomson scattering, and is nearly isotropic[7]

$$\frac{dI^R}{d\Omega} = \frac{3}{8\pi} \frac{6+\sin^2\beta}{10}. \tag{8}$$

TABLE I. Values used to calculate the Raman cross sections for gaseous nitrogen and oxygen. The values of γ at 1064 nm are extrapolated from experimental data.

	B_0 (m^{-1}) (Refs. 6, 8)	D_0 (m^{-1}) (Refs. 6, 8)	g_J (even J) (Ref. 6)	g_J (odd J) (Ref. 6)	$\gamma(10^{-30}\,m^3)$ (Refs. 6, 9, 10)
N_2	1.99×10^2	5.74×10^{-4}	6	3	0.66
O_2	1.44×10^2	4.73×10^{-4}	0	1	1.02

In the Raman calibration, we filled the LHD vacuum vessel with air and measured Raman signal intensity at six pressures upto 537 hPa to determine the quantity, S^R/n^{AIR}. The air pressure was monitored with a capacitance manometer installed on the LHD. Figure 3 shows the density dependence of the Raman signal detected by channel 1 in a polychromator. The Raman signals from 300 laser pulses were accumulated to decrease the statistical uncertainty. The signal intensity is proportional to the air density as expected. The calibration coefficients for each polychromator are obtained from the gradient of the fit line. The rejection of the filters at the laser wavelength is $>10^5$, however, stray light signal is observed at density zero since the stray light is very strong and the rejection is not complete.

Finally, we describe the estimation of uncertainties. The largest two errors are originated from the estimation of $\Sigma_J w_J^{N,O} \sigma_J^{N,O}(\lambda_J^{N,O}) f_1(\lambda_J^{N,O})$ that denotes the degree of overlapping of the spectral responsibility and Raman cross-section distribution. First, since the values of the polarizability anisotropy has uncertainties of ±4 and $\pm5\%$ for molecular nitrogen and oxygen, respectively, resulting in the cross-section uncertainties of $\pm8.4\%$. Second, the polychromators observe only the blue-wing of the Raman spectrum whose cross sections are small as shown in Fig. 2. Therefore, the value of $\Sigma_J w_J^{N,O} \sigma_J^{N,O}(\lambda_J^{N,O}) f_1(\lambda_J^{N,O})$ is very sensitive to

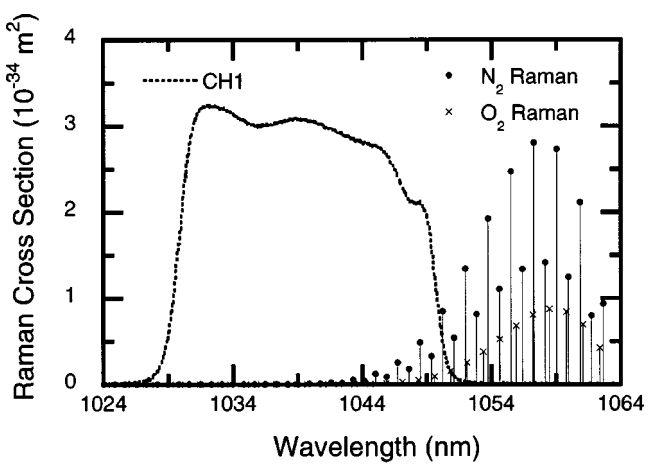

FIG. 2. Spectral responsibility of the channel 1 and effective Raman cross sections for molecular nitrogen and oxygen. The air is assumed to be composed with N_2 78 and O_2 21%.

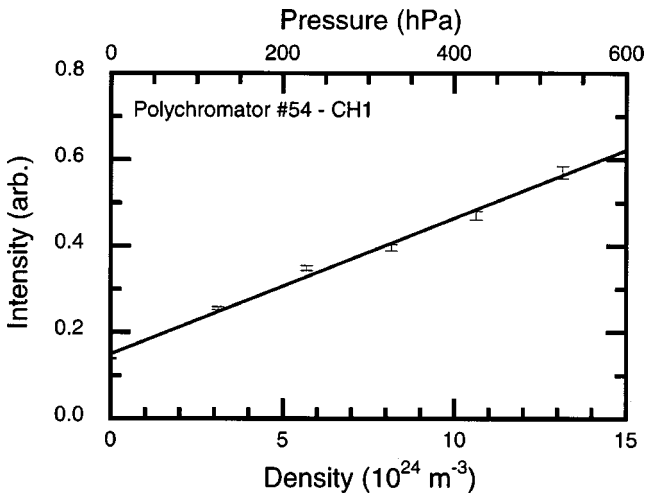

FIG. 3. Density dependence of the Raman signals measured by a polychromator. The calibration factor is defined by the gradient of the fit line.

the relative position of the spectral responsibility to Raman lines. The absolute wavelengths of the Raman transitions have been accurately established, however, the absolute position of the spectral responsibility includes some uncertainty. To decrease the uncertainty, we have carefully measured the spectral responsibility and the temperatures of the polychromators are stabilized with temperature-controlled, cooled water for suppressing the variations of the filter characteristics. We have estimated the uncertainty to be $\pm 7\%$. From the same reason, the error in $\int \sigma^T(T_e,\lambda) f_1(\lambda) d\lambda$ is expected to become larger for lower-electron temperature. The error increases rapidly smaller as the electron temperature increases and the Thomson spectrum becomes broader. The errors are estimated to be 4, 1, and 0.5% at 10, 50, and 100 eV, respectively. The error in the determination of the calibration factor S^R/n^{AIR} is $\pm 4\%$. Statistical uncertainty in S^T depends on the detected photon number of Thomson scattered light, and is typically $\pm 5\%$ or less. From the considerations above, total uncertainty has been estimated to be ± 12–15%, depending on electron temperature and density of plasmas.

III. ELECTRON-DENSITY MEASUREMENTS

With the calibrated YAG Thomson scattering, we have measured electron temperature and density profiles of LHD plasmas. First, as a critical check for the absolute densities measured by the YAG Thomson scattering, we evaluated the line densities from the density profiles, and compared with those obtained from the LHD millimeter-wave (MMW) interferometer.[11] The MMW interferometer measures line integrated electron density at a horizontal port as the YAG Thomson scattering, and so the line densities measured by the two diagnostics can be compared directly without any assumption. Figure 4 shows the comparison between line densities by the YAG Thomson scattering and the MMW interferometer. The plasma stored energy and time sequences of the heating devices are also plotted in the figure. It has been found that the line densities by the two diagnostics show fair agreements. In the plasma discharge, a pellet was injected at 1.0 s, and then the electron density jumped up significantly at the time. Both of the two density diagnostics observed the temporal behavior correctly. Figures 5(a)–5(d) show the electron density and temperature profiles of the plasma discharge at some selected times, which are also indicated in Fig. 4. It is noted that the Raman calibration has not yet been carried out for the polychromators that observe Thomson light scattered at the major radius of 2.5–2.8 m, and then density data have not obtained yet in the region whereas entire temperature profiles have been observed. It is noted that a simple extrapolation was used for estimating the line-integrated densities. The data scatters in the measured densities are somewhat larger than that for temperatures. This may be due to the fact that the temperatures are ob-

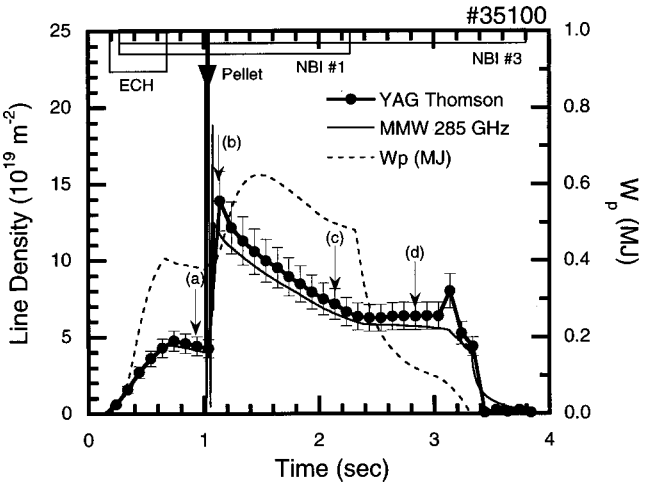

FIG. 4. Comparison between temporal evolutions of the line densities obtained from the YAG Thomson scattering and measured by the millimeter-wave interferometers. The rapid increase of density at 1.0 s is due to the pellet injection.

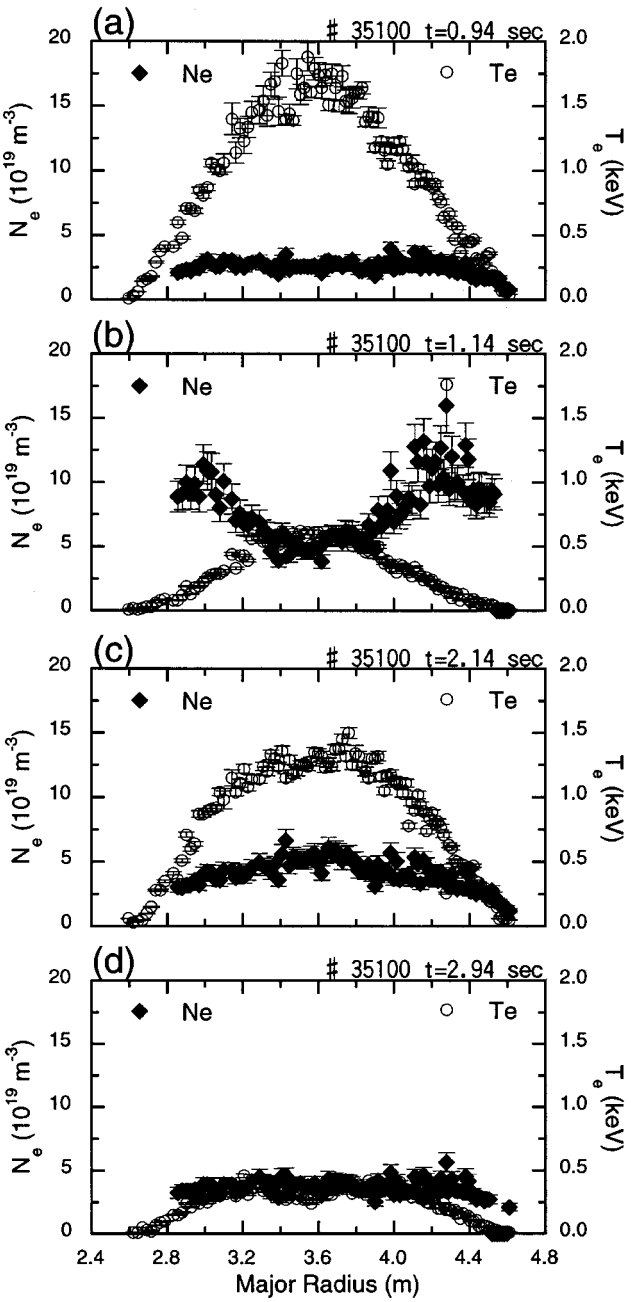

FIG. 5. (a)–(d). Time evolutions of electron temperature and density profiles. The observation times are also indicated in Fig. 4.

tained by using five wavelength channels, however we determine the densities from only one channel. The electron densities are increased just after the pellet injection, especially in the outer region, and the density profile changed from a trapezoidal shape to a remarkable hollow shape. After then, the density profiles become nearly parabolic as the temperature profile, and the electron temperature is increased again by two neutral beam heatings. After one neutral beam heating is terminated, the temperature decreases while the density is maintained. Such time history of the discharge is consistent with those by other LHD plasma diagnostics.

IV. CONCLUSIONS

We have successfully calibrated the LHD YAG Thomson-scattering system by using anti-Stokes rotational Raman scattering from air for which the fundamental scattering properties have been well established. The air Raman calibration is suited from a safety point of view, especially on large fusion devices. The line integrated electron densities obtained with the calibrated YAG Thomson scattering show good agreements with those measured by millimeter-wave interferometer. The detail temperature and density profiles measured by the calibrated LHD YAG Thomson scattering will serve important information on the physics of helical plasmas.

ACKNOWLEDGMENTS

The authors would like to acknowledge the contributions of the LHD experimental group. This research was partially supported by the Japan Society for the Promotion of Science, Grant-in-Aid for Scientific Research (B), 14380221, 2002.

[1] H. Röhr, Phys. Lett. **81**, 451 (1981).
[2] J. Howard, B. W. James, and W. I. B. Smith, J. Phys. D **12**, 1435 (1979).
[3] K. Narihara *et al.*, Fusion Eng. Des. **34-35**, 67 (1997).
[4] K. Narihara, I. Yamada, H. Hayashi, and K. Yamauchi, Rev. Sci. Instrum. **72**, 1122 (2001).
[5] T. Matoba, T. Itagaki, T. Yamauchi, and A. Funahashi, Jpn. J. Appl. Phys. **18**, 1127 (1979).
[6] C. M. Penny, R. L. St. Peters, and M. Lapp, J. Opt. Soc. Am. **64**, 712 (1974).
[7] R. W. Carlson and W. R. Fenner, Astrophys. J. **178**, 551 (1972).
[8] A. Weber, *Raman Spectroscopy of Gases and Liquid* (Springer, Berlin, 1979), p. 71.
[9] G. R. Alms, A. K. Burnham, and W. H. Flygare, J. Chem. Phys. **63**, 3321 (1975).
[10] N. J. Bridge and A. D. Buckinghum, Proc. R. Soc. London, Ser. A **295**, 334 (1966).
[11] K. Kawahata, K. Tanaka, Y. Ito, A. Ejiri, and R. J. Wylde, Rev. Sci. Instrum. **70**, 695 (1999).